ELSEVIER

Biophysical Chemistry 134 (2008) 56–63

Biophysical Chemistry

http://www.elsevier.com/locate/biophyschem

Mixing ratio-dependent energy transfer from DNA-bound 4′,6-diamidino-2-phenylindole to [Ru(1,10-phenanthroline)$_2$dipyrido[3,2-*a*:2′,3′-*c*]phenazine]$^{2+}$

Ji Yeon Choi [a], Jeong-Mi Lee [a], Hyosun Lee [b], Maeng Joon Jung [c], Seog K. Kim [a], Jong Moon Kim [a,*]

[a] *Department of Chemistry, Yeungnam University, Dae-dong, Gyeongsan City, Gyeong-buk, 712-749, Republic of Korea*
[b] *Department of Chemistry, Kyungpook National University, 1370 Sankyuk-dong, Buk-gu, Daegu, 702-701, Republic of Korea*
[c] *School of Applied Chemical Engineering, Sangju National University, Sangju City, Gyeong-buk, 742-711, Republic of Korea*

Received 28 September 2007; received in revised form 16 January 2008; accepted 17 January 2008
Available online 6 February 2008

Abstract

The binding mode of Δ- and Λ-[Ru(1,10-phenanthroline)$_2$dipyrido[3,2-*a*:2′,3′-*c*]phenazine]$^{2+}$ ([Ru(phen)$_2$DPPZ]$^{2+}$) to DNA in the presence of 4′,6-diamidino-2-phenylindole (DAPI) at a low and high [DAPI]/[DNA base] ratio (0.02 and 0.20, respectively) was investigated using electric absorption and circular dichroism spectroscopy. The spectral properties of both the Δ- and Λ-[Ru(phen)$_2$DPPZ]$^{2+}$ were not altered in the presence of DAPI disregarding the [DAPI]/[DNA] ratio, suggesting that the presence of DAPI in the minor groove of DNA does not affect the binding mode of the [Ru(phen)$_2$DPPZ]$^{2+}$ complex to DNA. The transferring excited energy of DAPI to both Δ- and Λ-[Ru(phen)$_2$DPPZ]$^{2+}$ occurs through Förster type resonance when they both spontaneously bound to DNA. At a high [DAPI]/[DNA] ratios, an upward bending curve in the Stern–Volmer plot, and a shortening the DAPI fluorescence decay time with increasing [Ru(phen)$_2$DPPZ]$^{2+}$ concentration were found. These results indicate that the quenching of the DAPI's fluorescence occurs through both the static and dynamic mechanisms. In contrast, the quenching mechanism at a low [DAPI]/[DNA] ratios was found to be purely static. The static quenching constant decreased linearly with respect to the [DAPI]/[DNA] ratio. Decrease in quenching efficiency can be explained by the association constant of [Ru(phen)$_2$DPPZ]$^{2+}$ to DNA while being within a quenchable distance from a DAPI molecule.

Keywords: DNA, 4′,6-diamidino-2-phenylindole; [Ru(1,10-phenanthroline)$_2$dipyrido[3,2-*a*:2′,3′-*c*]phenazine]$^{2+}$; Energy transfer; Spectroscopy; Luminescence

1. Introduction

The energy and the charge transfer between DNA-bound drugs or drug to DNA bases have been the subject of intensive studies. This interest is a result of the fact that stacked π-orbitals of DNA base pairs can serve as an effective medium for electron/charge transfer [1–8]. The reported biological importance of the charge transfer in DNA has been highlighted by the discovery of the oxidative damage done to DNA from a distance when inside the cell nucleus [9,10]. As well, an understanding of the charge transport in DNA has also been shown essential for developing nanodevices, i.e. designing a nanometer-sized self-assembling molecular wire [11–14].

In the electron/charge transfer experiments the DNA is often covalently or non-covalently modified by acceptor or donor molecules. It has been shown, the luminescence intensity of a DNA intercalator [Ru(1,10-phenanthroline)$_2$dipyrido[3,2-*a*:2′,3′-*c*]phenazine]$^{2+}$ (referred to as [Ru(phen)$_2$DPPZ]$^{2+}$, Fig. 1) was efficiently quenched by the presence of another intercalator, [Rh(9,10-diimine phenanthrenequinone)$_2$bypyridine]$^{3+}$ when they were simultaneously bound to a DNA molecule [15,16]. Alternatively, the quenching efficiency was significantly lower when, [Ru(NH$_3$)$_6$]$^{3+}$, a non-intercalating species was used. Furthermore, experiments have shown evidence for

* Corresponding author. Tel.: +82 53 810 3547; fax: +82 53 815 5412.
E-mail address: alex830@yumail.ac.kr (J.M. Kim).

0301-4622/$ - see front matter © 2008 Elsevier B.V. All rights reserved.
doi:10.1016/j.bpc.2008.01.006

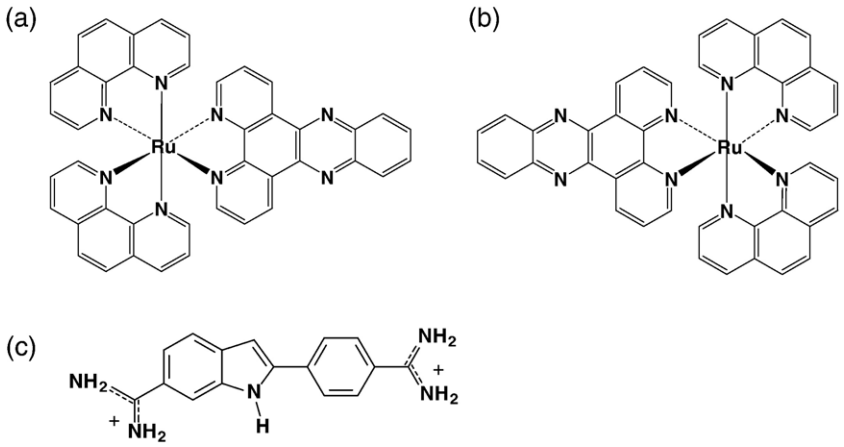

Fig. 1. Chemical structure of (a) Λ- and (b) Δ-$[Ru(phen)_2DPPZ]^{2+}$ and (c) DAPI.

the electron transfer along the DNA stem, by demonstrating the transfer of the excited energy between DNA-bound $[Ru(phen)_2DPPZ]^{2+}$ and Rh(III) complex occurs by electron transfer.

Electron transfer is not the only reason for this investigation of the interaction between these drugs bound to DNA. We were also interested in the binding mode and the efficiency of the electron and/or energy transfer, which are expected to be closely related. The binding mode of target drugs can be affected by the presence of alternate drugs either by blocking the binding sites, or by interactions between the different drugs. In previous experiments using circular dichroism (CD) and linear dichroism (LD) properties of *meso*-tetrakis(*N*-methylpyridinium-4-yl)porphyrin (referred to as TMPyP) and $[Ru(phen)_2DPPZ]^{2+}$, the drugs absorption to the AT-rich DNA were not altered [17–20]. Furthermore, it was also shown that even when the minor groove of DNA was blocked by 4′,6-diamidino-2-phenylindole (DAPI, hereafter, Fig. 1), which is a well-established as a minor groove binding drug, the adsorption of the drugs was not altered [21–26]. However, we propose a process in which direct energy transfer between DNA-bound drugs has been found. More specifically, excited energy of DNA was shown to be transferred to TMPyP [17] and $[Ru(phen)_2DPPZ]^{2+}$ [18–20] through Förster type resonance, in which DNA may be considered as a medium that holds two drugs within specific distance of each other. The observation of energy transfer between DNA to bound drugs is of interest because energy transfer reactions frequently occur along the electron transfer reaction pathways in biological systems. In this study, we report the mixing ratio-dependent energy transfer efficiency from a minor groove bound DAPI to Δ- and Λ-enantiomers of $[Ru(phen)_2DPPZ]^{2+}$ when they simultaneously bound to DNA. The mixing ratio, *r*, has been defined as the ratio of the concentration of DAPI to DNA base pair. At an extremely low mixing ratios, DAPI is expected to spread over the DNA minor groove leaving space and distance for incoming $[Ru(phen)_2DPPZ]^{2+}$ complexes. Alternatively, at high mixing ratios the DAPI molecules are in close vicinity to the Ru(II) complexes.

2. Materials and methods

2.1. Materials

Calf thymus DNA (referred to as DNA) was purchased from Worthington Biochemical Co (Lakewood, NJ). It was thoroughly dissolved at 4 °C in 5 mM cacodylate buffer, pH 7.0, containing 100 mM NaCl and 1 mM EDTA. The DNA solution was then dialyzed over several rounds against 5 mM cacodylate buffer, pH 7.0. The latter buffer was used throughout this work. The Λ- and Δ-$[Ru(phen)_2DPPZ]^{2+}$ were synthesized by reported methods [27]. The concentrations of the DNA, DAPI and $[Ru(phen)_2DPPZ]^{2+}$ were determined using spectroscopy, and utilizing the molar extinction coefficients of $\varepsilon_{258\ nm}$=6700 cm^{-1} M^{-1}, $\varepsilon_{342\ nm}$= 27,000 cm^{-1} M^{-1} and $\varepsilon_{439\ nm}$=20,000 cm^{-1} M^{-1}, respectively.

2.2. Spectroscopic measurements

Absorption and CD spectra were recorded on a Cary 100 (Victoria, Australia) and Jasco J 810 (Tokyo, Japan), respectively. CD spectra were averaged over an appropriate numbers of scans when necessary. Fluorescence spectra and intensities were measured using Jasco FP777. Fluorescence decay times of DNA-bound DAPI in the presence and absence of Λ- and Δ-$[Ru(phen)_2DPPZ]^{2+}$ were measured using IBH 5000U Fluorescence Life Time System (Glasgow, UK). The LED source of a nanoLED-03, which produces an excitation radiation at 370 nm with full width at half maximum of ~1.3 ns, was used to excite DNA-bound DAPI. The slit widths were 12 nm and 16 nm, respectively, for excitation and emission.

2.3. Fluorescence quenching

Fluorescence quenching is a process in which the fluorescence intensity of a given fluorophore decreases upon addition of quencher molecule [28]. When the mechanism of the fluorescence quenching follows either a simple static or a dynamic quenching model, a straight line is expected from the plot of the ratio of the

fluorescence intensity in the absence to the presence of quencher molecule (F_0/F) with respect to the quencher concentrations ([Q]). This relationship is explained in Eq. (1)

$$\frac{F_0}{F} = 1 + K_{SV}[Q]. \quad (1)$$

In this equation, the Stern–Volmer quenching constant, K_{SV}, is either a static (K_S) or a dynamic quenching constant (K_D). In the static process, the static quenching constant may be understood as an association constant for the formation of a non-fluorescent complex between the fluorophore and the quencher. In the dynamic process, the dynamic quenching constant is a multiple of the bimolecular quenching constant (k_q) and the fluorescence decay time in the absence of a quencher (τ_0). The Stern–Volmer plot observed in this work shows an upward bending curve for the fluorescence quenching of the DNA-bound DAPI by [Ru(phen)$_2$DPPZ]$^{2+}$ (see Results). Upward bending curve in the Stern–Volmer plot may be attributed either to a combined static–dynamic quenching process

$$\frac{F_0}{F} = (1 + K_S[Q])(1 + K_D[Q]) \quad (2)$$

$$\frac{F_0/F - 1}{[Q]} = (K_S + K_D) + K_S K_D[Q] \quad (3)$$

or to a sphere of action model, within which the quenching efficiency is unity.

$$\frac{F_0}{F} = (1 + K_D[Q]) \exp([Q]VN/1000) \quad (4)$$

$$\ln\left(\frac{F_0/F}{1 + K_D[Q]}\right) = \frac{VN}{1000}[Q]. \quad (5)$$

In Eqs. (4) and (5), V denotes the calculated volume of the sphere and N is the Avogadro's number. In this work, both the static–dynamic and the sphere of action models were tested.

3. Results

The fluorescence intensity of DNA-bound DAPI decreased upon addition of [Ru(phen)$_2$DPPZ]$^{2+}$. As it is shown in Fig. 2(a) the fluorescence emission spectrum of the DNA-bound DAPI at the [DAPI]/[DNA] ratio of 0.02 as well as 0.20 in both the presence and absence of 0.3 μM of Λ- or Δ-[Ru(phen)$_2$DPPZ]$^{2+}$. At this low mixing ratio, DAPI is expected to spread well in the minor groove of the DNA. The fluorescence intensity of DNA-bound DAPI at 450 nm decrease by the factor of 3.18 and 2.50 in the presence of Λ- or Δ-[Ru(phen)$_2$DPPZ]$^{2+}$, respectively. However, the contour of the emission spectrum remained unchanged in spite of the large decrease in the fluorescence intensity. As the [DAPI]/[DNA] ratio increased to 0.2, at which the minor groove of the DNA is considered to be saturated by the DAPI molecule, the fluorescence intensity of DNA-bound DAPI in the absence of Ru complexes is smaller by the factor of about 13 compared to that at a mixing ratio of 0.02 (Fig. 2(b)). The shape of the emission spectrum also changed at a high [DAPI]/[DNA] ratio in which the emission peak was found at 461 nm with a shoulder around at 510 nm. The addition of the [Ru(phen)$_2$DPPZ]$^{2+}$ complex to the DNA–DAPI complex at a high mixing ratios also resulted in a decrease in the fluorescence intensity. The extent of decrease in the fluorescence intensity at a high mixing ratio is smaller than that at a low mixing ratio: the fluorescence intensity decreased by the factor of 1.90 and 1.63 upon addition of 0.3 μM of Λ- or Δ-[Ru(phen)$_2$DPPZ]$^{2+}$, respectively. The shape of the fluorescence emission spectrum remained in the presence and absence of the [Ru(phen)$_2$DPPZ]$^{2+}$ as it was observed for the DNA–DAPI complex at a low [DAPI]/[DNA] ratio.

The [DAPI]/[DNA] ratio-dependent decreases in the fluorescence intensity of the DNA-bound DAPI with respect to increasing [Ru(phen)$_2$DPPZ]$^{2+}$ complex concentrations are depicted in Fig. 3(a) and (b) as a Stern–Volmer type plot according to Eq. (1). As seen from the figures, the quenching efficiency of both the Λ- or Δ-[Ru(phen)$_2$DPPZ]$^{2+}$ complexes for the DNA-bound DAPI increased as the ratio [DAPI]/[DNA] increased. The fluorescence quenching for the DNA-bound DAPI is more efficient for the Λ-[Ru(phen)$_2$DPPZ]$^{2+}$ complex compared to the Δ-enantiomer at all [DAPI]/[DNA] mixing

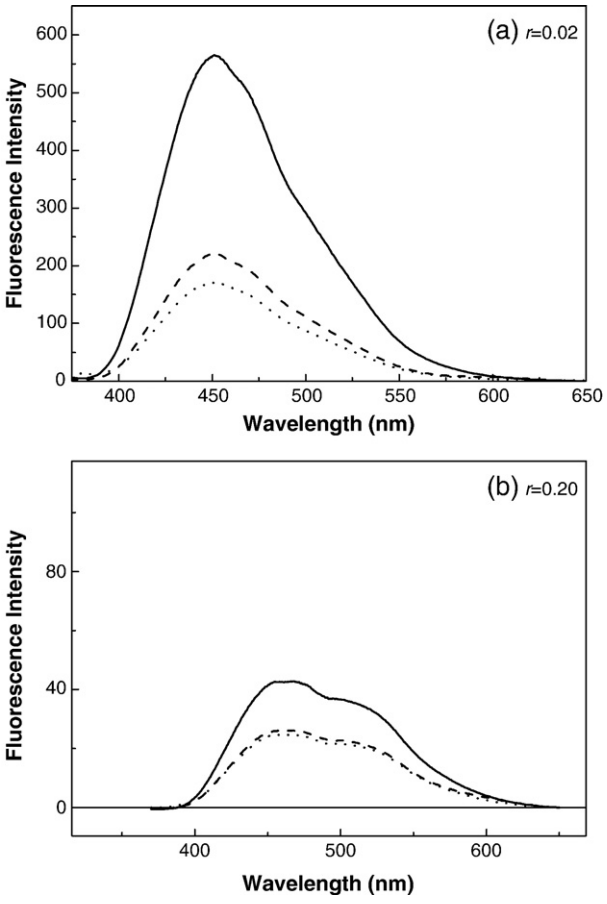

Fig. 2. The emission spectrum of DNA-bound DAPI at the mixing ratio of 0.02 (panel(a)) and 0.20 (panel(b)) in the absence (solid curve) and presence of Λ-(dotted curve) and Δ-[Ru(phen)$_2$DPPZ]$^{2+}$ (dashed curve). The DNA–DAPI complex was excited at 360 nm. Slit widths were 5/5 nm for both excitation and emission. The concentration of DNA was 10 μM, and that of the Ru(II) complex was 0.3 μM.

ratios. It is noteworthy that in the absence of DNA, the fluorescence intensity of DAPI did not change by adding the Ru (II) complex. Therefore, the quenching is heavily mediated by the DNA. In general, the Stern–Volmer plot appeared to be an upward banding curve for all [DAPI]/[DNA] ratios for both Λ- and Δ-$[Ru(phen)_2DPPZ]^{2+}$. The resulting upward bending curve in Stern–Volmer plot, Fig. 3, may be explained either by a mixed static–dynamic quenching model or by an inner sphere model. When analyzing the quenching property by either of the models the dynamic quenching constant is necessary.

The dynamic quenching constant can be obtained from the slope of the ratio of the fluorescence decay time in the presence of quencher to that in the absence (Fig. 4). In the absence of the Ru(II) complex, the fluorescence decay times of DNA-bound DAPI at the [DAPI]/[DNA] ratio of 0.02 were 0.90 ns and 3.59 ns with their relative amplitude of 0.106 and 0.894, respectively. At a [DAPI]/[DNA] ratio of 0.20, the decay times were shortened to 0.77 ns and 2.93 ns, with their relative amplitude of 0.329 and 0.671. The addition of the Ru(II) complexes resulted in further shortening in the decay times. For instance, the fluorescence decay time at the mixing ratio of 0.02 became 0.76 ns and 3.20 ns with their amplitude of 0.231 and 0.769, respectively, in the presence of 0.25 μM of Δ-$[Ru(phen)_2DPPZ]^{2+}$. The changes in the ratio of the average decay time in the absence of the quencher to its presence, $\langle\tau_0\rangle/\langle\tau\rangle$, versus the concentrations of the Ru(II) complexes is depicted in Fig. 4 for representative two extreme [DAPI]/[DNA] ratio of 0.02 and 0.20. In this plot, the average fluorescence decay time is defined by $\langle\tau\rangle=(a_1\tau_1^2+a_2\tau_2^2)/(a_1\tau_1+a_2\tau_2)$ for two decay components system where $\langle\tau\rangle$ is the average decay time, τ_is denote measured decay time components and a_is are corresponding relative amplitude. From the slopes, the dynamic quenching constants were calculated as $0.60\times10^6\ M^{-1}$ and $0.51\times10^6\ M^{-1}$, respectively, for Λ- and Δ-$[Ru(phen)_2DPPZ]^{2+}$; furthermore,

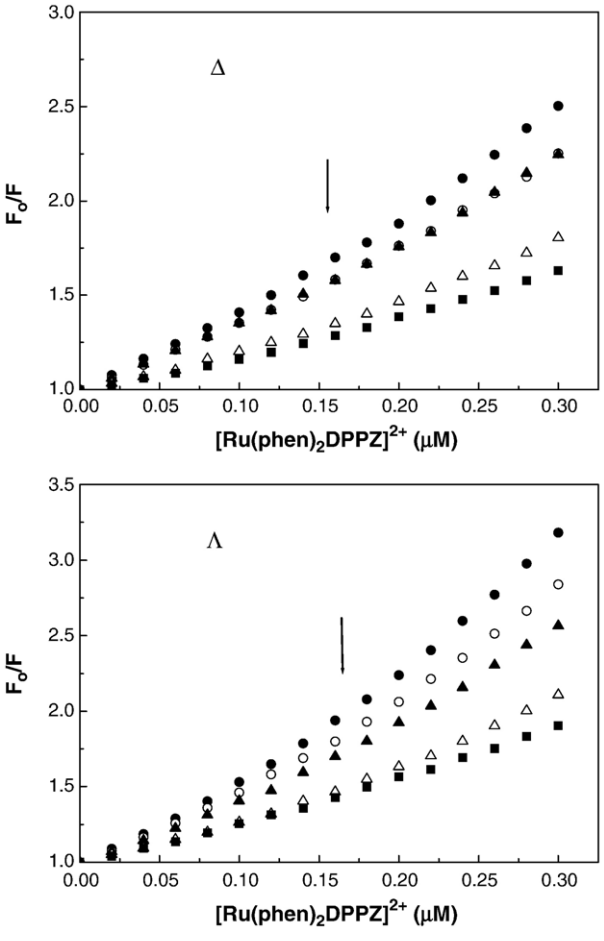

Fig. 3. The Stern–Volmer plot for the mixing ratio-dependent quenching of the DNA–DAPI complex fluorescence by Λ- and Δ-$[Ru(phen)_2DPPZ]^{2+}$, and [DNA]=10 μM. The [DAPI]/[DNA] ratios were plotted as 0.02 (filled circles), 0.05 (empty circles), 0.10 (filled triangles), 0.15 (empty triangle) and 0.20 (filled squares). The fluorescence intensities were measured at an excitation at 360 nm and an emission 450 nm, respectively. The slit widths were 5/5 nm for both excitation and emission.

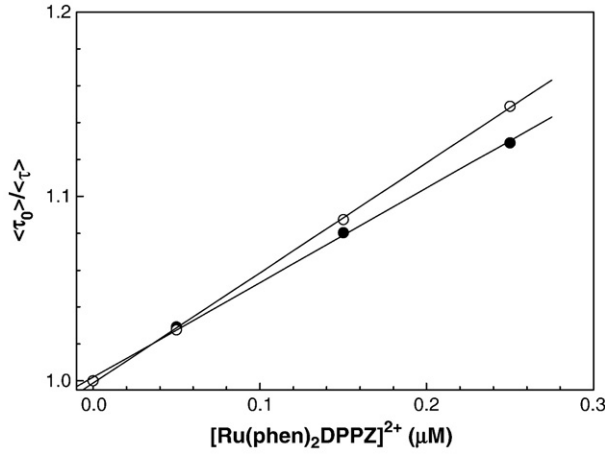

Fig. 4. A plot of the ratio of average fluorescence decay time of the DNA-bound DAPI in the absence to the presence of the quencher, $[Ru(phen)_2DPPZ]^{2+}$, with respect to the quencher concentration. Fluorescence decay time was measured by a 370 nm excitation and a 450 nm emission wavelength. The slit widths were 12/16 nm, respectively for excitation and emission with [DNA]=10 μM. The decay time was invariant of the mixing ratio. The filled circles represent the Δ, and empty circles represent the Λ-enantiomers of $[Ru(phen)_2DPPZ]^{2+}$.

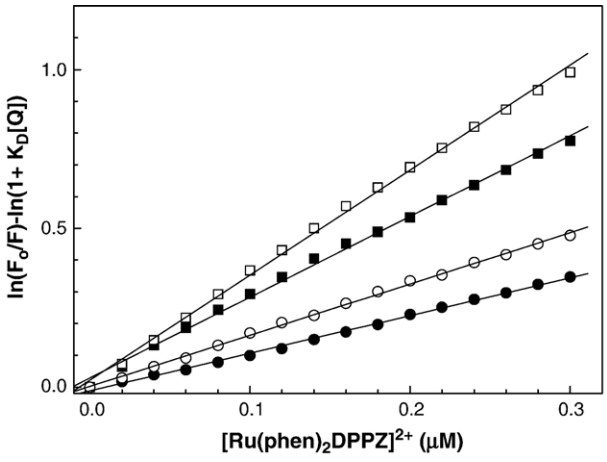

Fig. 5. The plot of $\ln\left(\frac{F_0/F}{1+K_D[Q]}\right)$ versus $\frac{VN}{1000}[Q]$, according to Eq. (5). This is intended to elucidate the sphere of action model. The slope and the radii of the sphere were calculated (see text). The squares represent the [DAPI]/[DNA]=0.02 with Δ-$[Ru(phen)_2DPPZ]^{2+}$ (closed square) and Λ-$[Ru(phen)_2DPPZ]^{2+}$ (open square), and the circles represents [DAPI]/[DNA]=0.20 with Δ-$[Ru(phen)_2DPPZ]^{2+}$ (closed circle) and Λ-$[Ru(phen)_2DPPZ]^{2+}$ (open circle).

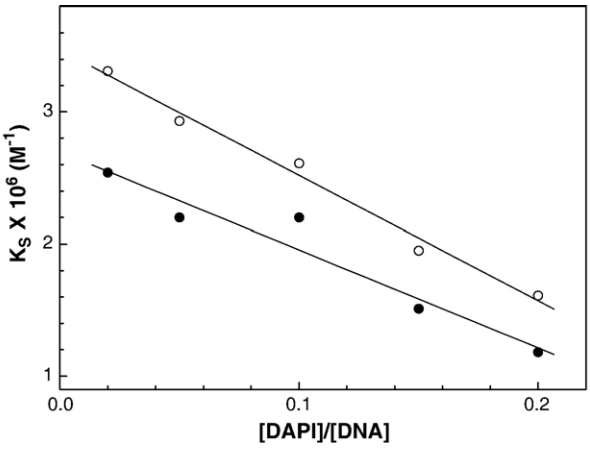

Fig. 6. A plot of the change in the static quenching constant in the quenching of DNA-bound DAPI fluorescence by Λ-(empty circles) and Δ-$[Ru(phen)_2DPPZ]^{2+}$ (filled circles). The static quenching constants, K_S, were obtained by combining the measured dynamic quenching constant and utilizing Eq. (3).

these dynamic quenching constants are invariant of the mixing ratios.

Using the measured dynamic quenching constant, and from the slopes of the plot of Eq. (5) which are shown in Fig. 5 for two extreme mixing ratios of the DNA–DAPI adducts, the volume of the sphere of action and the sphere radius between the drugs have been calculated. The resulting distances within which the quenching efficiency is unity were in the range of 7.78×10^4 Å (mixing ratio of 0.20, Δ-$[Ru(phen)_2DPPZ]^{2+}$) $\sim10.95\times10^4$ Å (mixing ratio of 0.02, Λ-$[Ru(phen)_2DPPZ]^{2+}$). These distances are unusually long compared to the normal sphere radius that is slightly larger than that of the sum of the radii of the fluorophore and quencher. A radius of few angstroms was reported from the quenching of $[Ru(phen)_2DPPZ]^{2+}$ in a non-aqueous solution by water [29]. The upward bending curve in the Stern–Volmer plots can also be analyzed by the combination of static and dynamic mechanisms according to Eq. (3). Using the measured dynamic quenching constant and Eq. (3), the static quenching constant can be obtained. This constant can be described as the association constant of the $[Ru(phen)_2DPPZ]^{2+}$ complex with DNA-bound DAPI. As it is shown in Fig. 6, the magnitude of static quenching constant decreased linearly with respect to the mixing ratio, and the ratio of the concentration of DNA-bound DAPI to DNA bases.

The absorption spectrum for DNA-bound DAPI and Δ-$[Ru(phen)_2DPPZ]^{2+}$ and that of the DNA–DAPI–Δ-$[Ru(phen)_2DPPZ]^{2+}$ complex at the [DAPI]/[DNA] ratio of 0.02 and 0.20, respectively, are shown in Fig. 7(a) and (b). Identical absorption spectra were recorded for the Λ-enantiomer, but are not shown in this paper. At both mixing ratios, DNA-bound DAPI exhibited an absorption maximum at 359 nm, which is consistent with reported values [21,22]. Two absorption bands with their maximum at 439 nm and 380 nm were apparent for DNA-bound $[Ru(phen)_2DPPZ]^{2+}$, which is also consistent with previous reports [27]. The former band, at 439 nm, is attributed to the MLCT band of the Ru(II) complex, and the latter, at 359 nm, to DPPZ ligand absorption band. It has been shown that DAPI and $[Ru(phen)_2DPPZ]^{2+}$ bound to DNA simultaneously shows absorption spectrum characterized by two maximum at 366 nm and 439 nm. The subtraction of the absorption spectrum of DNA-bound $[Ru(phen)_2DPPZ]^{2+}$ from that of the DNA–DAPI–Δ-$[Ru(phen)_2DPPZ]^{2+}$ complex resulted in the identical absorption spectrum to that of DNA-bound DAPI at both low and high [DAPI]/[DNA] ratios (insertions). This result indicates that the binding of one drug to DNA does not affect to the binding mode of another drug; as it was previously observed with poly[d(A-T)$_2$] at a high binding density [18–20]. The CD spectra under similar conditions are depicted in Fig. 8. At the [DAPI]/[DNA] ratio of 0.02, DNA-bound DAPI exhibited a positive band at 340 nm, which is attributed to DAPI that bind in the minor groove of DNA. Conversely, the CD spectrum of the DNA-bound DAPI at a mixing ratio of 0.20, a positive band at 366 nm with a small negative envelope near 415 nm has shown an interaction. This species of DAPI has been shown to

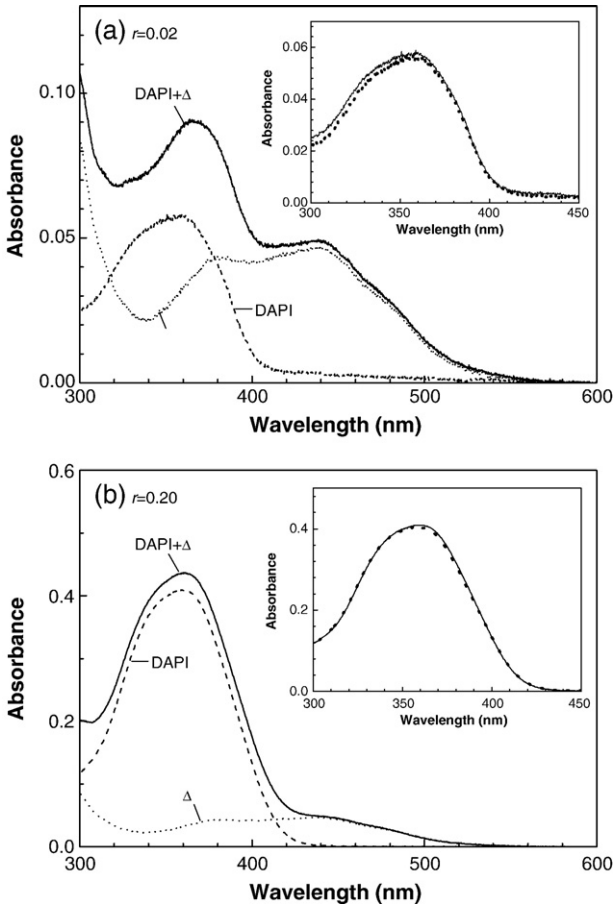

Fig. 7. The resulting absorption spectrum of DAPI (dashed curve), Δ-$[Ru(phen)_2DPPZ]^{2+}$ (dotted curve) and Δ-$[Ru(phen)_2DPPZ]^{2+}$–DAPI mixture (solid curve) in the presence of DNA at the [DAPI]/[DNA] = 0.02 (panel a) and 0.20 (panel b); with [DNA] = 100 μM and [Δ-$[Ru(phen)_2DPPZ]^{2+}$] = 3 μM. The Λ-enantiomer exhibited exactly the same spectra. After insertion: absorption spectrum of DNA-bound DAPI (solid curve) and the that of DAPI (dotted curve) that constructed by subtraction from the absorption spectrum of DNA-bound Δ-$[Ru(phen)_2DPPZ]^{2+}$ from the DAPI, Ru(II) complex and DNA mixture. For all spectra, the absorption spectrum of DNA was subtracted.

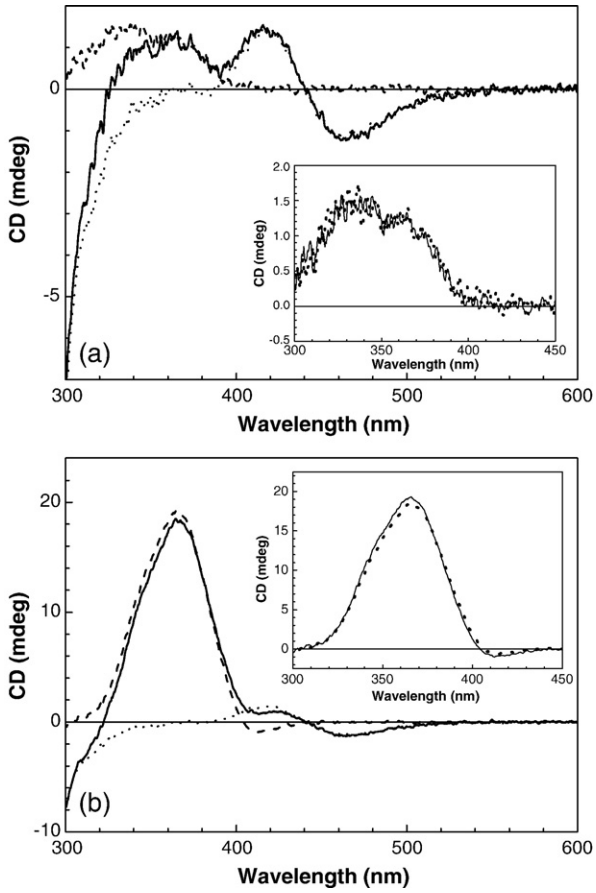

Fig. 8. The CD spectrum of DAPI (dashed curve), Δ-$[Ru(phen)_2DPPZ]^{2+}$ (dotted curve) and Δ-$[Ru(phen)_2DPPZ]^{2+}$–DAPI mixture (solid curve) in the presence of DNA at the [DAPI]/[DNA]=0.02 (panel a) and 0.20 (panel b). The conditions and curve assignment are the same as in Fig. 6.

interact with the DNA in the minor groove when at a high binding density [22]. When the CD spectrum of DNA-bound Δ-$[Ru(phen)_2DPPZ]^{2+}$ was subtracted from that of the DNA–DAPI–Δ-$[Ru(phen)_2DPPZ]^{2+}$ complex, the resulting CD spectrum is identical with that of the DNA-bound DAPI (insertion) both at low and high mixing ratios. The CD spectrum of DNA-bound DAPI at both low and high [DAPI]/[DNA] ratios were also identical in the presence and absence of Λ-$[Ru(phen)_2DPPZ]^{2+}$ and results are not shown.

4. Discussion

4.1. The effect of DAPI on the binding of Δ-$[Ru(phen)_2DPPZ]^{2+}$ to DNA

It has been shown that the spontaneous binding of DAPI and $[Ru(phen)_2DPPZ]^{2+}$ complex does not affect their DNA binding modes. Therefore, the spectral properties of DNA-bound DAPI are not affected by the presence of the $[Ru(phen)_2DPPZ]^{2+}$ complex, and those of the DNA-bound $[Ru(phen)_2DPPZ]^{2+}$ complex are not altered by the presence of DAPI. Similar observations have been reported for the poly[d(A-T)$_2$]–DAPI–$[Ru(phen)_2DPPZ]^{2+}$ complex system. Although the extended DPPZ ligand is undoubtedly intercalated between DNA base pairs in the complex formed between DNA and $[Ru(phen)_2DPPZ]^{2+}$, the direction of insertion, i.e., whether from the minor groove or from the major groove has been debated. The intercalation from the major groove for $[Ru(phen)_2DPPZ]^{2+}$ was shown by ^{1}H NMR NOE data [30]. However, alteration at the minor groove either by formation of a triplex [31] or by glycosylation [32] resulted in the same spectral properties of the $[Ru(phen)_2DPPZ]^{2+}$ complex when compared to the duplex DNA suggesting that the insertion direction is toward the minor groove. Recent ^{1}H NMR studies also support that the $[Ru(phen)_2DPPZ]^{2+}$ binds towards the minor groove [33,34]. However, all possible binding sites at the minor groove of DNA conceivably are blocked under the conditions of this work because more than 99% of the amount of the DAPI added can be considered as bound species according to the stability constants at the present ionic strength [35,36]. One DAPI molecule has been reported to occupy about 5 DNA base pairs at the DNA minor groove [21–26,37]. Therefore, the fact that the spectral properties of both Λ- and Δ-$[Ru(phen)_2DPPZ]^{2+}$ remain even at a [DAPI]/[DNA] ratio of 0.20 suggests that there is no interaction between them at the ground-state. This observation supports the major groove as the insertion direction of the $[Ru(phen)_2DPPZ]^{2+}$ complex, as it was reported for poly[d(A-T)$_2$] [18–20].

The association constant for the binding of the $[Ru(phen)_2DPPZ]^{2+}$ complex to DNA has been reported to be in the $5–6\times10^6$ M^{-1} [27]. The association constants measured for both Δ- and Λ-$[Ru(phen)_2DPPZ]^{2+}$ to DNA at a low [DAPI]/[DNA] ratio obtained from modified Stern–Volmer method (Fig. 5) are 2.54×10^6 and 3.31×10^6, respectively. Those at the [DAPI]/[DNA] ratio of 0.20 were slightly lower being 1.18×10^6 and 1.61×10^6, respectively, for Δ- and Λ-$[Ru(phen)_2DPPZ]^{2+}$. Therefore, although the spectral properties of the bound species are not affected each other, it is suggestive that the presence of DAPI may disturb the binding of both enantiomers of the Ru(II) complex to DNA. Since the spectral change properties remain, change in the DNA conformation near the DAPI binding site cannot be the reason for the lower binding affinity. Therefore, a simple decrease in the available binding sites for the Ru(II) complex by the pre-occupied DAPI may cause the decrease in the binding affinity.

The two binding modes of DAPI to DNA have been shown in the [DAPI]/[DNA] ratios adopted in this work namely, types I and II [21,22]. In the type I binding mode, which is represented by a positively induced CD spectrum in the DAPI absorption region with its maximum near 340 nm in which DAPIs are well-separated in the minor groove of the DNA. The interaction between DNA-bound DAPI is negligible, and the space between DAPI is wide. The CD spectrum observed in this work at [DAPI]/[DNA] ratio of 0.02 is the type I. The origin of the type II CD spectrum, for which the positive CD maximum at ~375 nm is apparent, is believed to be either a change in the DNA conformation at the DAPI binding site or to be the interaction between electric transitions between densely bound DAPI molecules. Whether DAPI is well-separated, or they interact with each other, the binding mode of DAPI is not

altered by the presence of any $[Ru(phen)_2DPPZ]^{2+}$ enantiomers. These observations support that DPAI binds at the minor groove of DNA while the DPPZ ligand of the $[Ru(phen)_2DPPZ]^{2+}$ complex inserts at the major groove.

4.2. Energy transfer from DAPI to Λ- and Δ-$[Ru(phen)_2DPPZ]^{2+}$

The energy transfer from DAPI to $[Ru(phen)_2DPPZ]^{2+}$ bound to a poly[d(A-T)$_2$] at a high binding density has been reported [18–20]. When the poly[d(A-T)$_2$]-bound DAPI complex was excited, the luminescence quantum yield of the $[Ru(phen)_2DPPZ]^{2+}$ complex, increased. It is believed that this complex binds at the major groove of poly[d(A-T)$_2$] at a high DAPI binding density. From this observation, the excited energy of DAPI can transfer across the DNA stem to $[Ru(phen)_2DPPZ]^{2+}$ that locates at the opposite side of the DNA. The origin of this energy transfer was suggested to be of Förster type resonance, in which the emission wavelength region of DNA-bound DAPI is overlapped with the MLCT absorption band of the Ru(II) complex. Similar energy transfer was found for DAPI–$[Ru(phen)_2DPPZ]^{2+}$–DNA system at a high binding density. According to the Förster type resonance energy transfer model, the distance between donor and acceptor as well as their relative orientation are the important factors that govern the efficiency. Considering the size of intercalated DPPZ and binding geometry, DAPI and $[Ru(phen)_2DPPZ]^{2+}$ are practically in contact as it was in poly[d(A-T)$_2$]. Therefore, the difference in the efficiency of the energy transfer between Δ- and Λ-enantiomers may be attributed to the different orientation of the intercalated DPPZ ligand relative to the DNA helix axis. Considering the high efficiency in the energy transfer compared to that of the low [DAPI]/[DNA] ratios, the excited energy of DAPI that is located some distance from bound $[Ru(phen)_2DPPZ]^{2+}$ can also be transferred.

The efficiency of the energy transfer is significantly lower at a low [DAPI]/[DNA] ratio and the difference between the enantiomers becomes less important. Therefore, in this case, the distance between the complexes is an important factor. At a given DAPI concentration, one DAPI molecule is bound per 50 base pairs, therefore it occupies five per 25 base pairs because binding of one DAPI molecule covers five base pairs. Then the center of DAPI binding site is in average 11 base pair, or ~37 Å, apart from the $[Ru(phen)_2DPPZ]^{2+}$ intercalation site. The average distance (the possible longest distance) between DAPI and the Ru(II) complex estimated here is reasonable because the binding of DAPI may disrupt, or at least not affect, the binding of $[Ru(phen)_2DPPZ]^{2+}$ as it was shown by the association constant. Although the estimate from the inner sphere model is unrealistically long, the excited energy of DAPI can certainly be transferred to $[Ru(phen)_2DPPZ]^{2+}$ which is at ~11 base pairs, or ~37 Å apart.

Acknowledgment

This work was supported by Korea Science and Engineering Foundation (Grant No. R01-2005-000-10490-0).

References

[1] M.E. Núñez, J.K. Barton, Probing DNA charge transport with metallointercalators, Curr. Opin. Struct. Biol. 4 (2000) 199–206.
[2] E.M. Boon, J.K. Barton, Charge transport in DNA, Curr. Opin. Struct. Biol. 12 (2002) 320–329.
[3] C.R. Treadway, M.G. Hill, J.K. Barton, Charge transport through a molecular p-stack: double helical DNA, Chem. Phys. 281 (2002) 409–428.
[4] S.D. Wettig, D.O. Wood, P. Aich, J.S. Lee, M-DNA: a novel metal ion complex of DNA studied by fluorescence techniques, J. Inorg. Biochem. 99 (2005) 2093–2101.
[5] T. Takada, K. Kawai, S. Tojo, T. Majima, Hole transfer in DNA: DNA as a scaffold for hole transfer between two organic molecules, Tetrahedron Lett. 44 (2003) 3851–3854.
[6] V.D. Lakhno, V.B. Sultanov, B.M. Pettitt, Combined hopping–superexchange model of a hole transfer in DNA, Chem. Phys. Lett. 400 (2004) 47–53.
[7] J. Rak, J. Makowska, A.A. Voityuk, Effect of proton transfer on the electronic coupling in DNA, Chem. Phys. 325 (2006) 567–574.
[8] A. Sadowska-Aleksiejew, J. Rak, A.A. Voityuk, Effects of intra base-pairs flexibility on hole transfer coupling in DNA, Chem. Phys. Lett. 429 (2006) 546–550.
[9] M.E. Núñez, G.P. Holmquist, J.K. Barton, Evidence for DNA charge transport in the nucleus, Biochemistry 40 (2001) 12465–12471.
[10] M.E. Núñez, K.T. Noyes, J.K. Barton, Oxidative transport through DNA in nucleosome particles, Chem. Biol. 9 (2002) 403–415.
[11] S.O. Kelly, N.M. Jackson, M.G. Hill, J.K. Barton, Long range electron transfer through DNA films, Angew. Chem. Int. Ed. 38 (1999) 941–945.
[12] A. Vainrub, B.M. Pettitt, Thermodynamics of association to a molecule immobilized in an electric double layer, Chem. Phys. Lett. 323 (2000) 160–166.
[13] S.J. Park, T.A. Taton, C.A. Mirkin, Array-based electrical detection of DNA with nanoparticle probes, Science 295 (2002) 1503–1506.
[14] D. Porath, G. Cuniberti, G.R. Di Felice, in: G.B. Shuster (Ed.), Topics in Current Chemistry, vol. 237, Springer, Berlin, 2004, pp. 183–228.
[15] C.J. Murphy, M.R. Arkin, M.R.Y. Jenkins, N.D. Ghatlia, S. Bossmann, N.J. Turro, J.K. Barton, Long-range photoinduced electron transfer through a DNA helix, Science 262 (1993) 1025–1029.
[16] C.J. Murphy, M.R. Arkin, N.D. Ghatlia, S. Bossmann, N.J. Turro, J.K. Barton, Fast photoinduced electron transfer through DNA intercalation, Proc. Natl. Acad. Sci. USA 91 (1994) 5315–5319.
[17] B. Jin, H.M. Lee, Y.-A. Lee, J.H. Ko, C. Kim, S.K. Kim, Simultaneous binding of *meso*-tetrakis(*N*-methylpyridinium-4-yl)porphyrin and 4',6-diamidino-2-phenylindole at the minor grooves of poly(dA)×poly(dT) and poly[d(A-T)$_2$]: fluorescence resonance energy transfer between DNA bound drugs, J. Am. Chem. Soc. 127 (2005) 2417–2424.
[18] B.W. Lee, S.J. Moon, M.R. Youn, J.H. Kim, H.G. Jang, S.K. Kim, DNA mediated energy transfer from 4',6-diamidino-2-phenylindole to $[Ru(1,10\text{-phenanthroline})_2L]^{2+}$, Biophys. J. 85 (2003) 3865–3871.
[19] B.H. Yun, J.-O. Kim, B.W. Lee, P. Lincoln, B. Nordén, J.-M. Kim, S.K. Kim, Simultaneous binding of Ruthenium(II)[$(1,10\text{-phenanthroline})_2$ dipyridophenazine]$^{2+}$ and minor groove binder 4',6-diamidino-2-phenylindole to poly[d(A-T)$_2$] at high binding densities: observation of fluorescence resonance energy transfer across the DNA stem, J. Phys. Chem. B. 107 (2003) 9858–9864.
[20] M.R. Youn, S.J. Moon, B.W. Lee, D.-J. Lee, J.-M. Kim, S.K. Kim, C.-S. Lee, DNA mediated energy transfer from 4',6-diamidino-2-phenylindole to Ru(II)$[(1,10\text{-phenanthroline})_2L]^{2+}$: effect of ligand structure, Bull. Korean Chem. Soc. 26 (2005) 537–542.
[21] B. Nordén, S. Erkisson, S.K. Kim, M. Kubista, R. Lyng, B. Åkerman, in: B. Pullman, J. Jortner (Eds.), Molecular Basis of Specificity in Nucleic Acid–Drug Interactions, Kluwer Acad. Pub., Netherlands, 1990, pp. 23–41.
[22] S. Eriksson, S.K. Kim, M. Kubista, B. Nordén, Binding of 4',6-diamidino-2-phenylindole (DAPI) to AT regions of DNA: evidence for an allosteric conformational change, Biochemistry, 32 (1993) 2987–2998.
[23] H.-K. Kim, J.-M. Kim, S.K. Kim, A. Rodger, B. Nordén, Interactions of intercalative and minor groove binding ligands with triplex

poly(dA)·[poly(dT)]$_2$ and with duplex poly(dA)·poly(dT) and poly[d(A-T)]$_2$ studied by CD, LD, and normal absorption, Biochemistry 35 (1996) 1187–1194.

[24] S. Mohan, N. Yathindra, Flexibility of DNA in 2:1 drug–DNA complexes-simultaneous binding of two DAPI molecules to DNA, J. Biomol. Struct. Dyn. 9 (1992) 695–704.

[25] E. Trotta, E. D'Ambrosio, N. Del Grosso, G. Ravagnan, M. Cirilli, M. Paci, 1H NMR study of [d(GCGATCGC)]$_2$ and its interaction with minor groove binding 4',6-diamidino-2-phenylindole, J. Biol. Chem. 268 (1993) 3944–3951.

[26] D. Vlieghe, J. Sponer, L. Van Meervelt, Crystal structure of d(GGCCAATTGG) complexed with DAPI reveals novel binding mode, Biochemistry 38 (1999) 16443–16451.

[27] C. Hirot, P. Lincoln, B. Noedén, DNA binding of delta- and lambda-[Ru(phen)$_2$DPPZ]$^{2+}$, J. Am. Chem. Soc. 115 (1993) 3448–3454.

[28] J. R. Lakowiz, in Principles of Fluorescence Spectroscopy, 2nd ed., Plenum Publisher, New York, 2001, pp. 237–249.

[29] R.B. Nair, B.M. Cullum, C.J. Murphy, Optical properties of [Ru(phen)$_2$dppz]$^{2+}$ as a function of nonaqueous environment, Inorg. Chem. 36 (1997) 962–965.

[30] C.M. Dupureur, J.K. Barton, Use of selective deuteration and ^{1}H NMR in demonstrating major groove binding of D-[Ru(phen)$_2$dppzI^{2+} to d(GTCGAC)$_2$, J. Am. Chem. Soc., 116 (1994) 10286–10287.

[31] S.-D. Choi, M.-S. Kim, S.K. Kim, P. Lincoln, E. Tuite, B. Nordén, Binding mode of [ruthenium(II) (1,10-phenanthroline)$_2$L]$^{2+}$ with poly (dT*dA-dT) triplex: ligand size effect on third-strand stabilization, Biochemistry 36 (1997) 214–223.

[32] E. Tuite, P. Lincoln, B. Nordén, Photophysical evidence that delta- and lambda-[Ru(phen)$_2$(dppz)]$^{2+}$ intercalate DNA from the minor groove, J. Am. Chem. Soc. 119 (1997) 239–240.

[33] A. Greguric, I.D. Greguric, T.W. Hambley, J.R. Aldrich-Wright, J.G. Collins, Minor groove intercalation of D-[Ru(Me$_2$phen)$_2$dppz]$^{2+}$ to the hexanucleotide d(GTCGAC)$_2$, J. Chem. Soc. Dalton Trans. 24 (2002) 849–855.

[34] J.G. Collins, J.R. Aldrich-Wright, I.D. Greguric, P.A. Pellegrini, Binding of the D- and l-enantiomers of [Ru(dmphen)$_2$dpq]$^{2+}$ to the hexanucleotide d(GTCGAC)$_2$, Inorg. Chem. 38 (1999) 5502–5509.

[35] G. Manzini, M.L. Barcellona, M. Avitable, F. Quadrifoglio, Interaction of diamidino-2-phenylindole (DAPI) with natural and synthetic nucleic acids, Nucleic Acids Res. 11 (1983) 8861–8876.

[36] W.D. Wilson, F.A. Tanious, H.J.K. Barton, L. Strekowski, D.W. Boykin, Binding of 4',6-diamidino-2-phenylindole (DAPI) to GC and mixed sequences in DNA: intercalation of a classical groove-binding molecule, J. Am. Chem. Soc. 111 (1989) 5008–5009.

[37] T.A. Larsen, D.S. Goodsell, D. Cascio, K. Grzeskowiak, R.E. Dickerson, The structure of DAPI bound to DNA, J. Biomol. Struct. Dyn. 7 (1989) 477–491.